Ligand variations in ReX(diimine)(CO)(3)] complexes: Effects on photocatalytic CO2 reduction

Kurz, Philipp; Probst, Benjamin; Spingler, Bernhard; Alberto, Roger

Abstract: Two series of complexes MX(diimine)(CO)(3)] (M = Tc, Re) have been prepared, fully characterised and investigated for their ability to act as photocatalysts for the reduction of CO2 to CO. One series consists of complexes with different aromatic diimine ligands while keeping X = Br- constant. The second series describes complexes with diimine = 2,2-bipyridine and variations in the anionic ligand X-. Although numerous complexes of this type have been prepared and investigated before, a systematic study of their photocatalytic activity has not yet been carried out. Electrochemical and spectroscopic characterisation of these complexes has been performed with the objective of better understanding their respective activity in the photocatalytic CO2 reduction. Despite various modifications, catalytic activity is retained for all compounds exhibiting fluorescence, including (TcCl)-Tc-99(bipy)(CO)(3)], whereas nonfluorescing compounds did not convert CO2 to CO. The correlation of catalytic activity and spectroscopic or electrochemical properties such as absorption or emission wavelengths, redox potentials or Stern-Volmer constants for the reductive quenching of the excited complexes is difficult. Nevertheless, the study emphasises the possibility to obtain ReX(CO)(3)(diimine)] complexes with a wide range of physicochemical properties by ligand variations and the great potential of compounds of this class of complexes as inorganic photosensitisers.

DOI: https://doi.org/10.1002/ejic.200600166

Metal and Ligand Variations in [MX(diimine)$(CO)_3$] (M=Tc, Re) Complexes: Effects on Photocatalytic CO_2 Reduction

Philipp Kurz, Bernhard Spingler and Roger Alberto

Institute of Inorganic Chemistry, University of Zürich, Winterthurerstrasse 190, 8057 Zürich, Switzerland.

ariel@aci.unizh.ch

Keywords: Photocatalysis / CO_2 reduction / Rhenium / Technetium/ Diimine Ligands

Abstract

Two series of complexes [MX(diimine)$(CO)_3$] (M = Tc, Re) have been prepared, fully characterized and investigated for their ability to act as photocatalysts for the reduction of CO_2 to CO . One series consists of complexes with different aromatic diimine ligands while keeping X = Br^- constant. The second series describes complexes with diimine = 2,2-bipyridine and variations in the anionic ligand X^-. Although numerous complexes of this type have been prepared and investigated before, a systematic study of their photocatalytic activity has not yet been carried out. Electrochemical and spectroscopic characterization of these complexes has been performed with the objective of better understanding their respective activity in the photocatalytic CO_2 reduction. Despite various modifications, catalytic activity is retained for all compounds exhibiting fluorescence, including [^{99}TcCl(bipy)$(CO)_3$], whereas non-fluorescing compounds did not convert CO_2 to CO. The correlation of catalytic activity and spectroscopic or electrochemical properties such as absorption or emission wavelengths, redox potentials or Stern-Volmer constants for the reductive quenching of the excited complexes is difficult. Nevertheless, the study emphasises the possibility to obtain [ReX$(CO)_3$(diimine)] complexes with a wide range of physicochemical properties by ligand variations and the great potential of compounds of this class of complexes as inorganic photosensitisers.

Introduction

The development of a system for the conversion of solar energy into chemical fuel is one of the most demanding challenges chemists face today. The choice of the photosensitiser performing the initial step of light absorption is of key importance. Complexes of the type $[Ru(diimine)_3]^{2+}$ have been most thoroughly studied in this respect.[1-4] Among further possible candidates, rhenium tricarbonyl diimine complexes $[ReX(diimine)(CO)_3]$ have also attracted broad interest.[5-14] The complex $[ReCl(phen)(CO)_3]$ was one of the first rhenium(I) carbonyl compounds ever synthesised.[15] Detailed studies have unveiled the remarkable photochemical properties of $[ReCl(phen)(CO)_3]$ and related compounds such as $[ReX(bipy)(CO)_3]$ ($X=Cl^-$ **1**, $X=Br^-$ **2**).[5, 9, 16, 17] The excited state generated by visible light absorption at 450 to 500 nm has been identified as a metal to ligand charge transfer (MLCT) state, with the photoelectron ejected from a metal centered π-d into a vacant ligand centered π* orbital with up to μsec lifetimes. On the basis of the Rehm-Weller approximation[18] the photoexcited molecules are powerful oxidising agents with potentials of +500 to +1200mV (vs. Ag/AgCl).[6] Thermodynamically, $[ReX(diimine)(CO)_3]$ complexes can therefore oxidise very poor electron donors, even H_2O, in their excited states, which makes them very interesting compounds for light - energy conversion.

In a marked contrast to the large number of physico-chemical investigations, there are only few examples of light-driven reactions with these complexes as photosensitisers. Most prominent is a system for the photochemical reduction of CO_2 developed in Strasbourg over 20 years ago. Hawecker *et al.* found that **1** and **2** are both able to act as photosensitiser and reduction catalysts for the two-electron conversion of CO_2 to CO transferring reduction equivalents from poor reducing agents like triethanolamine (TEOA, $\Delta E^\circ_{1/2} = + 0.8V$) (Scheme 1).[10, 19] In this "Strasbourg system", the energetically uphill, two-electron reduction process is achieved using the energy of absorbed visible light. From the initial experiments on, the mechanism of this unprecedented reaction has been of great interest.[8, 10, 20, 21] Many experiments have been carried out with the original catalysts **1** or **2**, but studies of the catalytic performance with variations in the anion X^- or the diimine ligand N∩N are rare.[13, 20]

Scheme 1

We present in this study the synthesis and characterisation of two series of $[ReX(diimine)(CO)_3]$ complexes and an investigation of the respective ligand effects on the photocatalytic activities. In a first series of complexes $[ReX(bipy)(CO)_3]$ (**4**-**7**), also including the Tc(I) analogue $[TcCl(bipy)(CO)_3]$ **3**, the bipy ligand is kept constant and X is varied. In a second series of

[ReBr(diimine)$(CO)_3$] (**8**-**15**), the Br^- ligand is kept constant but the diimine ligand is altered. The selected diimine ligands are depicted in Scheme 2. The detailed study of these series of complexes showed that the influence of both diimine and terminal X^- ligands on physicochemical and catalytic properties is large. Nevertheless, catalytic activity is retained in most cases.

Results and Discussion

Synthesis and Characterisation. The complexes [$ReBr(CO)_5$] and $(NEt_4)_2$[$ReBr_3(CO)_3$] are convenient starting materials from which [ReBr(diimine)$(CO)_3$] complexes are directly afforded with the diimine ligands shown in Scheme 2. The Tc(I) complex **3** was prepared similarly from $(NEt_4)_2$[$TcCl_3(CO)_3$]. For the synthesis of the [ReX(bipy)$(CO)_3$] series, $[Re(bipy)(CO)_3(sol)]^+$ was prepared as an intermediate by halide precipitation and in a consecutive step the ligands X = OH_2 (**4**), SCN^- (**5**) or CN^- (**6**) were introduced. Treatment of **4** with only half an equivalent of cyanide gave the dinuclear complex **7** in which two Re centres are linked by a cyanide bridge with a Re-Re distance of 5.4 Å.[22]

Scheme 2

Structures. All complexes depict an octahedral ligand arrangement with a facial tricarbonyl moiety, a bidentate diimine ligand and an anion X. The structure of the Tc surrogate **3** of the original photocatalyst **1** is shown in Figure 1 and complex **10** with the most extended ligand dppz in Figure 2. In all cases the two equatorial carbonyl ligands, the rhenium centre and aromatic rings of the diimine ligand are in a nearly ideal planar arrangement. Bond lengths and angles around the metal centers (see supplementary information) are similar for all structures and well comparable to those in closely related compounds.[23-25]

Figure 1 and Figure 2

For the biquinoline (biq) complex **11** the usual planar arrangement of metal centre, diimine ligand and equatorial CO's was not observed. The aromatic rings of biq are displaced from the otherwise favoured $Re(CO)_2$- plane by 23° and 12°, respectively, due to steric strain between the hydrogen atoms of the outer aromatic rings and the equatorial carbonyl ligands (Figure 3). Similar biq complexes show comparable structural features.[26] The different twist angles for the two quinoline rings seem to be an effect of crystal packing since only six ^1H NMR signals are observed, indicating equivalence for the biq rings on the NMR timescale in solution.

Figure 3

Spectroscopic properties. Table 1 summarises analytical data obtained for the [ReX(bipy)$(CO)_3$] series of complexes. Variation of ligand $X^{(-)}$ causes clear effects, but a correlation between $X^{(-)}$ and the spectroscopic or electronic data of the corresponding complexes is not readily obvious. The exchange of Br^- for water results in the formation of the cationic complex **4**. As a consequence of its charge, **4** has the series' lowest reduction potential and its light absorption shifts towards higher energy, as it is more difficult to excite an electron. The π- backbonding is reduced in **4** and the IR vibrations ν_{CO} shift to higher wavenumbers. The mono-cation **7** fits in this series with respect to the ν_{CO} frequencies, however $E_{1/2}$ is larger than for e.g. **5**. Considering ν_{CO}, the thiocyanate complex **5** appears to be about as low in electron density as **4**, yet its visible absorption is shifted the most towards lower energies. The cyano complex has the smallest CO wavenumbers indicating high electron density on Re(I) but also a low wavelength of light absorption.

Table 1

Much larger differences in spectroscopic properties are observed when the diimine ligand is altered (Table 2). The carbonyl stretching frequencies vary by only about ± 5 cm^{-1} for all the complexes, thus, the electron density on Re(I) does not seem to be as greatly affected as in the case of the [ReX(bipy)$(CO)_3$] series. The differences in the spectroscopic properties stem from the decreased energy of the diimine's LUMO when going to larger aromatic systems or heteroatom substitution.[1, 16] The shift in λ_{max} towards smaller energies causes a larger part of the absorption to be in the visible for complexes like **10**, **11** or **15** (Figure 4). While all other compounds are orange yellow solids, **11** and **15** are deep red and dark blue-green, respectively. For **11**, this might be explained by the effect of the unusual coordination geometry on the electronics of the molecule. In the case of **15**, the exceptionally low-lying, particularly stabilized LUMO of this ligand has already been reported to cause unusual absorption properties of abpy- complexes.[27]

Table 2

According to Table 2, not all of the complexes exhibit room temperature fluorescence in DMF when irradiated with light between 350 and 450 nm (Figure 5). The emission maxima are between 520 and 585 nm for **2**, **8**, **9**, **10** and **12,** but **11**, **13**, **14** and **15** do not fluoresce. This behaviour is

rationalized in **11** and **15** by the small energy gap between ground and excited states as indicated by the high values of λ_{max}. Accordingly, radiationless decay to the ground state will be fast in accordance with the energy gap law.[18] Other reasons must account for the absence of fluorescence in **13** and **14** as the energy gap is similar to the structurally related complexes **2** and **8**, respectively. The emission of the dppz complex **10** is observed at much lower wavelengths (520nm) than that of all other fluorescing complexes of this study. Due to the special nature of the dppz ligand, both diimine and phenazine centered excited states are theoretically possible[28], resulting in the observation of MLCT or LC emissions, respectively. It was found in a recent study of closely related complexes of $[Re(CO)_3Cl]$ with 11- substituted dppz that the ligand centred emission is dominating for two 11-X-dppz complexes of rhenium tricarbonyl[25], thus explaining the unusual emission behaviour observed for **10**.

Figure 4 and Figure 5

Electrochemistry. Reversible, one-electron reduction is observed for all complexes except **12** (Figure 6). This process has been assigned to a ligand centred reduction resulting in the formation of what is best described as a rhenium(I) organic radical anion species $[ReX(CO)_3(diimine^{\bullet -})]$.[11] In agreement with the spectroscopic properties, the exchange of the ligand X influences the reduction potential $E_{1/2,red}$ of the complexes far less than the variation of the diimine (Tables 1 and 2).

Factors changing $E_{1/2,red}$ are the overall charge of the complex and the size of the aromatic system of the diimine. In the $[ReX(CO)_3bipy]$ series, cationic **4** is the one most easily reduced. Similarly, the reduction of the cationic dinuclear cyano complex **7** is more facile compared to e.g. the neutral complex **6**. It is furthermore easier to place an additional electron into the LUMO of a large aromatic ligand, as seen for the $[ReBr(CO)_3(diimine)]$ series for which the reduction potential of the complexes increases with the size of the diimine ligand.

Remarkable redox behaviour was found for **14** and **15**. Complex **15** shows a very high reduction potential of $E_{1/2,red}$= +50 mV as the additional electron is localised in its unusual LUMO at the azo-bridge.[29] The electrochemistry of **14**, its molecular structure shown in Figure 6, is special since the phd ligand is formally an *ortho*-benzoquinone system. The first reduction occurs already at –15 mV and generates a strongly stabilized semiquinone radical. The diolate is formed at –755mV in a second reversible step. Increasing concentrations of H_2O shift the second reduction to higher potentials, as direct two-electron reduction to the diol is known to occur in in the presence of protons (Figure 7).[30] The phd complex **15** thus offers the possibility of a reversible storage of two electrons within a range of accessible potentials, which is unique within this series of rhenium diimine complexes.

Figure 6 and Figure 7

Reductive fluorescence quenching. The original work on the "Strasbourg system" suggested that the primary events of reaction are photoexitation of the complex followed by the reaction of the thexi- state with the electron donor.[8, 10, 21] It was therefore of interest how the synthetic modifications of the catalyst influence the ability of the excited complexes to react with the standard electron donor TEOA.

Fluorescence quenching is a good way to probe the reactions of the excited state with electron donors (see supporting information). For all fluorescing complexes, STERN-VOLMER kinetics are observed for the reductive quenching by TEOA in DMF solutions. According to the STERN-VOLMER equation, constants K_{SV} can be determined from plots of (I_0/I)-1 versus quencher concentration (Figure 8):[18]

$$\mathbf{I_0/I = 1 + k_q \tau [Q] = 1 + K_{SV} [Q]}$$

Figure 8 and Table 3

Table 3 summarises the determined K_{SV} values which are indicators for the "success rate" of forming the reduced complex after photoexcitation in the presence of quencher. The variations of diimine or X^- cause K_{SV} to vary by a factor of up to five. To explain this result, measurements of the excited state lifetimes τ would be necessary to estimate differences in the bimolecular quenching reaction rate k_q. It is known that the k_q of this reaction can vary at least up to a factor of 2.5 for a series of much more closely related $[ReX(CO)_3bipy]$ compounds[13]. Unfortunatly, we did not have access to an instrument for fluorescence decay measurements.

A number of experiments were carried out to probe the possibility of finding a different solvent/ donor combination for which reductive fluorescence quenching is observed. Fluorescence quenching of **2** by either TEOA or TEA is also found in acetonitrile or acetonitrile/water solutions, but the K_{SV} values found in these systems are smaller than in DMF by a factor of 2 and 5, respectively. The use of ternary amines as sacrificial electron donors restricts the reactions to alkaline conditions. This is a particular disadvantage for the goal of shifting the reactivity from CO_2 to H_2O reduction, as H_2O reduction is thermodynamically more difficult under basic or neutral conditions. Therefore other, non-basic electron donors with irreversible oxidation between +0.5 to +1 V and solubility in DMF, MeCN or H_2O where studied. Well suited candidates are oxalic acid, vitamin C, cystamine or EDTA.[31] None of these donors did cause any quenching of

[ReX(diimine)$(CO)_3$] fluorescence in solution, although all meet the requirements of a thermodynamically accessible, irreversible oxidation. [31]

Photochemical CO_2 reductions. Experiments to study the photocatalytic activity of these complexes in the Strasbourg system were carried out under conditions similar to the reported set-up.[10] Only CO but no detectable quantities of H_2 were found in the head space of the reaction solutions.

Figure 9

The time course of produced CO per mole of catalyst for the [ReX(bipy)$(CO)_3$] series and the technetium homologue **3** are shown in Figure 9. All complexes of this series are active catalysts, though at very different rates (Table 4). It is most interesting to note that after a significant change of the metal center - from rhenium to technetium - catalytical activity was retained. The thiocyanato complex **5** is a better catalyst than the original complexes **1** and **2** as it combines a rate as fast as **1**, but with improved long-term stability, as the turnover rate for **5** does not change over the first two hours. The reason for this enhanced stability might be the suppression of the formation of the catalytically inefficient formato complex [Re(HCOO)(bipy)$(CO)_3$][10] as undesired side product in reactions catalysed by **1** or **2**. The complexes of the larger diimines (**8**, **9** and **10**) are all active photocatalysts but at smaller rates than **2** (Table 4). No CO or any other gaseous products were detected for reactions using **11**, **13**, **14** or **15**. Thus, there is a strict correlation between the detection of room temperature fluorescence and catalytic activity: all fluorescing complexes are active catalysts for photocatalytic CO_2 reduction while the others are not.

In agreement with the fluorescence quenching experiments described earlier, the same experiments with different donors such as cystamine or vitamin C in DMF gave no CO. Furthermore, it has been claimed in the literature that the system would switch from CO_2 to H_2O reduction if the reaction was carried out in a THF/water mixture instead of DMF.[32] We tried to reproduce this result multiple times with our catalysts but no product at all, neither H_2 nor CO, was detected in a THF / water (4:1) mixture. On the other hand, about half the rate of CO production was observed with **2** in DMF / 10% water.

Table 4

These results support the original catalytic mechanism proposed by the Strasbourg group.[10] The well established initial step is the absorption of a visible-light photon by the catalyst [$Re^{I}X$(diimine)$(CO)_3$] and subsequent MLCT to form the excited state [$Re^{II}X$(diimine$^{\bullet-}$)$(CO)_3$].

This step occurs for all complexes discussed here but for **11**, **13**, **14** and **15** nonradiative relaxation pathways to the ground state are most probably so fast that no consecutive reactions can occur, as the absence of fluorescence for these compounds indicates. Hence, they are inactive as Strasbourg catalysts regardless of their electro- or photochemical properties.

According to our results, there is no evidence to support a carboxylate-bridged rhenium dimer as key intermediate, as proposed in a recent study[14], as this is in disagreement with the pronounced influence observed for the terminal ligands in the [ReX(bipy)$(CO)_3$] series. Also, the different compounds act both as photoactive and catalytic centres for the reduction of CO_2, but none does show any reactivity to reduce water, as has been claimed before.[32]

Conclusion

We could show in this study that the [ReX(bipy)$(CO)_3$] catalysts for the Strasbourg system can easily be modified. The catalytic activity for photocatalytic reduction of CO_2 is retained in most cases or even enhanced, even though spectroscopic and electrochemical properties of the complexes are substantially altered. There are, however limitations to the degree to which the diimine ligand can be varied. For a group of [ReBr$(CO)_3$(diimine)] compounds, catalytic activity is lost together with the ability of these complexes to fluoresce, indicating that a sufficiently long excited state life-time is of course a key prerequisite for photoreactivity. While many of the rhenium complexes are able to catalyse the two-electron photoreduction of CO_2, none shows any reactivity for the reduction of the much more important substrate H_2O. Nevertheless, the unusual reactivity of [ReX$(CO)_3$(diimine)] compounds, observed once more in this study, justifies that they should be considered to a larger extend as promising alternatives to the [Ru(diimine$)_3]^{2+}$ class of compounds.

Experimental section

General. All chemicals were of reagent grade and used without further purification. Water was doubly distilled before use. Synthetic reactions were carried out under N_2 using standard Schlenk techniques. Abbreviations of the diimine ligands are according to Scheme 2. The complexes [ReBr$(CO)_5$][33], $(NEt_4)_2$[ReBr$_3(CO)_3$][34] and $(NEt_4)_2$[TcCl$_3(CO)_3$][35], [ReCl(bipy)$(CO)_3$][36] (**1**), [ReBr(bipy)$(CO)_3$][36] (**2**), [ReBr(phen)$(CO)_3$][37] (**8**), [ReBr(biq)$(CO)_3$][38] (**11**) as well as the ligands abpy[39], dpq[40], dppz[41] and phd[42] were synthesized according to published procedures. Preparations of the complexes **4**[43], **5**[44], **6**[45], **7**[45], **13**[37] and **15**[46] have been reported before in the literature but for this study these compounds were obtained via the different, in most cases more facile, routes described below.

Caution! ^{99}Tc is a weak β-emitter with a half-life of 2.12 x 10^5 years. Although radiation from small amounts of material is absorbed completely by the walls of the glassware, reactions should only be carried out in specially equipped laboratories and under well-ventilated hoods.

[^{99}TcCl(bipy)(CO)$_3$] (**3**). $(NEt_4)_2[^{99}TcCl_3(CO)_3]$ (33 mg, 0.06 mmol) was stirred in 5 ml of H_2O for 2 h, bipy (15.5 mg, 0.1 mmol) was added, dissolved in a mixture of EtOH (1 ml) and H_2O (2 ml). After 30 min a yellow precipitate started to form, which was filtered off after a reaction time of 12 h, washed with ether and dried in *vacuo*. Yield: 18 mg (80%). IR (KBr, cm^{-1}): ν_{CO} = 2031 (s), 1944 (s), 1920(s); ν_{bipy} = 1601 (m), 1469(m), 1441 (m), 771 (m). ^{1}H NMR (MeOH-*d*$_4$): δ 9.03 (br, 2H), 8.63 (d, 2H), 8.28 (m, 2H), 7.75 (m, 2H); ^{99}Tc NMR (MeOH-*d*$_4$) δ -1094.0 (s).

[Re(H$_2$O)(bipy)(CO)$_3$](OTf) (**4**). [ReBr(bipy)(CO)$_3$] (150 mg, 0.3 mmol) was dissolved in 15 ml of acetone and 76.1 mg AgOTf (1 eq.) acetone (5ml) were added. The mixture was heated to 70°C for 2 h. AgBr was filtered off and the solvent was removed in *vacuo*. The yellow residue was suspended in water (20 ml) and stirred at room temperature for 3 h. Insoluble parts were filtered off and the yellow solution was lyophilized to obtain the yellow, slightly hydroscopic product. Yield: 105 mg (60%). λ_{max} (DMF): 350 nm (*sh*, ε=4000), 553 nm (ε=1500). IR (KBr, cm^{-1}) ν_{CO} = 2036 (s), 1918 (s); ν_{bipy} = 1604 (m), 1475(m), 1447 (m), 771 (m); ν_{OTf} = 1291 (m), 1230 (m), 1179 (m). ESI-MS (acetone/MeOH): *m/z* = 427 [(M-H$_2$O)$^+$]. ^{1}H NMR (MeOH-*d*$_4$) δ 9.17 (m, 2H), 8.70 (m, 2H), 8.39 (m, 2H), 7.82 (m, 2H).

[Re(SCN)(bipy)(CO)$_3$] (**5**). **2** (50.6 mg, 0.1 mmol) was dissolved acetone (5 ml) and 17.1 mg AgOTf (1 eq.) in acetone (2 ml) were added. The mixture was heated to 70°C for 2 h. AgBr was filtered off and the solvent removed in *vacuo*. The residue was stirred MeOH (10 ml) for 1 h. KSCN (20 mg, 2 eq.), dissolved H_2O (2 ml), was added and the mixture heated to 70 °C for 4 h to obtain a clear yellow solution. The product precipitated after 1 d at 4 °C. The yellow compound was filtered off, washed with cold H_2O, MeOH and ether and dried in *vacuo*. Yield: 30 mg (60%). λ_{max} (DMF): 376 nm (ε=2500). λ_{em} (DMF): 580 nm. IR (KBr, cm^{-1}) ν_{SCN} = 2093 (s); ν_{CO} = 2020 (s), 1928 (s), 1914 (s); ν_{bipy} = 1602 (m), 1471(m), 1444 (m), 765 (m). ESI-MS (acetone/MeOH): *m/z* = 485 [M$^+$]. ^{1}H NMR (acetone-*d*$_6$) δ 9.15 (m, 2H), 8.77 (m, 2H), 8.42 (m, 2H), 7.86 (m, 2H).

[Re(CN)(bipy)(CO)$_3$] (**6**). $(NEt_4)_2[ReBr_3(CO)_3]$ (100 mg (0.13 mmol) were dissolved in H_2O (5 ml) and 66.2 mg (3 eq.) $AgNO_3$ in 3 ml of H_2O added. The solution was stirred at room temperature for 30 min before AgBr was removed by filtration. Bipy (20.3 mg, 1 eq.), dissolved in EtOH (2 ml) was added. HPLC analysis confirmed the quantitative formation of $[Re(H_2O)(bipy)(CO)_3]^+$ after 12h. Addition of KCN (25.4 mg, 3 eq.) and by 20 h of stirring at 100°C, resulted in the quantitative conversion to **6**, as detected by HPLC. The solvent was removed in *vacuo* and the product obtained by extraction of the residue with three 5 ml portions of THF. Yield: 45 mg (75%). λ_{max} (DMF): 354 nm (ε=2300). λ_{em} (DMF): 540 nm. IR (KBr, cm^{-1}) ν_{CN} = 2117 (w); ν_{CO} = 2006 (s), 1878 (s); ν_{bipy} =

1603 (m), 1473 (m), 1445 (m), 775 (m). ^{1}H NMR (acetone-d_6) δ 9.07 (d, 2H), 8.21 (d, 2H), 8.07 (m, 2H), 7.54 (m, 2H).

[(Re(bipy)(CO)$_3$)$_2$(μ-CN)](ClO$_4$) (**7**). $(NEt_4)_2[ReBr_3(CO)_3]$ (100 mg, 0.13 mmol) were dissolved in H_2O (10 ml) and 80.8 mg (3 eq.) $AgClO_4$ added. AgBr was removed after 30 min by filtration. Bipy (20.3 mg, 1 eq.), dissolved in 5 ml of EtOH was added. After 20 h at room temperature $[Re(bipy)(CO)_3(H_2O)]^+$ formed quantitatively, 4.2 mg KCN (0.5 eq.) in H_2O (2 ml) were added. After 2 h at 100°C, a yellow precipitate started to form which was filtered off after 20 h, washed with H_2O and ether and dried in *vacuo*. Yield: 28 mg (45%). λ_{max} (DMF): 363nm (ε=2000). λ_{em} (DMF): 535nm. IR(KBr, cm^{-1}) ν_{CN} = 2151 (w); ν_{CO} = 2025 (s), 1910 (s), 1896 (s); ν_{bipy} = 1605 (m), 1473 (m), 1446 (m), 771 (m); ν_{ClO4} = 1121 (m). ^{1}H NMR (acetone-d_6) δ 8.83 (br, 4H), 8.00 (br, 4H), 7.60 (br, 4H), 7.41 (br, 4H).

[ReBr(dpq)(CO)$_3$] (**9**). A procedure similar to the published method for the preparation of $[ReBr(phen)(CO)_3]$ was applied.[37] A suspension was prepared consisting of $[ReBr(CO)_5]$ (50 mg, 0.12 mmol) and dpq (28.5 mg, 1 eq.) in 10 ml of petroleum benzene (bp. 100-130°C). The suspension was heated to 100 °C for 2 h to obtain the product as a yellow precipitate. The powder was filtered off, washed with portions of petroleum benzene and ether and then dried in *vacuo* to obtain the product as a yellow powder. Yield: 70 mg (quantitative). λ_{max} (DMF): 400 nm (*sh*, ε=2500). λ_{em} (DMF): 585nm. IR (KBr, cm^{-1}) ν_{CO} = 2025 (s), 1948 (s), 1902 (s); ν_{dpq} = 1402 (m), 1384 (m), 820 (w), 729(w), 631 (w). ESI-MS (MeOH): *m/z* = 531 $[M\text{-}Br+CO]^+$, 503 $[M\text{-}Br]^+$. ^{1}H NMR (acetone-d_6) δ 9.96 (m, 2H), 9.82 (m, 2H), 9.38 (s, 2H), 8.45 (m, 2H).

[ReBr(dppz)(CO)$_3$] (**10**). The same procedure as for $[ReBr(dpq)(CO)_3]$ was applied, using $[ReBr(CO)_5]$ (50 mg, 0.12 mmol) and dppz (33.8 mg, 1 eq.), to obtain the complex as an orange powder. Yield: 50 mg (65%). λ_{max} (DMF): 400 nm (*sh*, ε=5000). λ_{em} (DMF): 520nm. IR (KBr, cm^{-1}) ν_{CO} = 2018 (s), 1918 (s), 1890 (s); ν_{dppz} = 1493 (m), 1418 (m), 1384 (m), 1360 (m), 822 (w), 773 (w), 729 (w). ESI-MS (MeOH): *m/z* = 581 $[M\text{-}Br+CO]^+$, 553 $[M\text{-}Br]^+$. ^{1}H NMR ($CDCl_3$) δ 10.04 (m, 2H), 9.88 (m, 2H), 8.47 (m, 2H), 8.08 (m, 2H), 7.26 (m, 2H). Anal. Calcd. For $C_{21}H_{10}BrN_4O_3Re$ (%): C, 39.88; H, 1.59; N, 8.86. Found: C, 39.53; H, 1.77; N, 8.58.

(NEt$_4$)[ReBr(Hdcbipy)(CO)$_3$] (**12**). $(NEt_4)_2[ReBr_3(CO)_3]$ (154 mg, 0.2 mmol) was dissolved in 15 ml of H_2O and H_2dcbipy (53.7 mg, 1.1 eq.) was added as a solid. The pH of the solution was raised to pH~6-7 by the careful addition of 10 mM NaOH. The mixture was stirred for 2 d at room temperature and some yellow precipitate formed, which was filtered off. The filtrate was lyophilized, triturated three times with 5 ml of CH_2Cl_2 to remove NEt_4Br and then dried in *vacuo*. Yield: 75 mg (50%). IR (KBr, cm^{-1}) ν_{CO} = 2024 (s), 1896 (s); ν_{dcbipy} = 1719 (w), 1619 (m), 1551 (w), 1366 (m), 1289 (m), 1071 (w), 766 (m), 682 (m). ESI-MS (MeOH): *m/z* = 569 $[(M\text{-}COOH\text{-}H)^-]$. ^{1}H NMR ($D_2O/Na_2CO_3$) δ 9.05 (m, 2H), 8.67 (m, 2H), 7.82 (m, 2H).

[ReBr(bpm)(CO)$_3$] (**13**). $(NEt_4)_2[ReBr_3(CO)_3]$ (385 mg, 0.5 mmol) was dissolved in 20 ml of H_2O and bpm (87 mg, 1.1 eq.), dissolved in 2 ml of EtOH was added. The mixture was stirred for 2 d at room temperature, after which a fine orange precipitate had formed. The solid was filtered off, washed with H_2O, cold EtOH and ether, and dried in *vacuo*. Yield: 210 mg (80%). λ_{max} (DMF): 383 nm (ε=2500). IR (KBr, cm^{-1}) ν_{CO} = 2030 (s), 1931 (s), 1906 (s); ν_{bpm} = 1575 (m), 1547 (w), 1407 (s), 834 (w), 755 (w). ESI-MS (acetone/MeOH): *m/z* = 508 [M^+]. ^{1}H NMR (acetone-d_6) δ 9.41 (dd, 2H), 9.36 (dd, 2H), 7.98 (dd, 2H).

[ReBr(phd)(CO)$_3$] (**14**). The same procedure as for [ReBr(bpm)(CO)$_3$] was applied, using $(NEt_4)_2[ReBr_3(CO)_3]$ (500 mg, 0.65 mmol) and phd (163 mg, 1.2 eq.) to isolate the orange complex. Yield: 350 mg (95%). λ_{max} (DMF): 375 nm (*sh*, ε=3000). IR (KBr, cm^{-1}) ν_{CO} = 2033 (s), 1943 (s), 1885 (s); ν_{phd} = 1703 (m), 1573 (w), 1427 (m), 1298 (w), 1026 (w), 828 (w), 727 (w). ESI-MS (MeOH): *m/z* = 512 [$(M\text{-}Br+MeO)^+$], 480 [$(M\text{-}H\text{-}Br)^+$]. ^{1}H NMR (acetone-d_6) δ 9.34 (dd, 2H), 8.81 (dd, 2H), 8.05 (dd, 2H). Anal. Calcd. For $C_{15}H_6BrN_2O_5Re$ (%): C, 32.15; H, 1.08; N, 5.00. Found: C, 32.37; H, 1.12; N, 5.08.

[ReBr(abpy)(CO)$_3$] (**15**). The same procedure as for [ReBr(bpm)(CO)$_3$] was applied, using $(NEt_4)_2[ReBr_3(CO)_3]$ (76 mg, 0.1 mmol) and abpy (27 mg, 1.5 eq.) to isolate the violet-blue compound. Yield: 50 mg (95%). λ_{max} (DMF): 361 nm (ε=5000), 553 nm (ε=1500). IR (KBr, cm^{-1}) ν_{CO} = 2020 (s), 1924 (s), 1900 (s); ν_{abpy} = 1465 (w), 1433 (m), 1370 (w), 797 (m). ESI-MS (acetone/MeOH): *m/z* = 533 [$(M\text{-}H)^+$], 454 [$(M\text{-}H\text{-}Br)^+$]. ^{1}H NMR (acetone-d_6) δ 9.33 (m, 1H), 8.96 (m, 1H), 8.87 (m, 1H), 8.57 (td, 1H), 8.20 (br, 2H), 8.00 (br, 1H), 7.85 (br, 1H). Anal. Calcd. For $C_{13}H_8BrN_4O_3Re$ (%): C, 29.22; H, 1.51; N, 10.49. Found: C, 29.61; H, 1.43; N, 10.56.

Physical Measurements. UV-Vis spectra were measured using a Cary 50 spectrometer with solution samples in 1cm quartz cells. If necessary, cells with silicon septa lids were used to keep samples under an inert gas atmosphere during measurements. Fluorescence measurements were performed on a Perkin Elmer LS50B fluorescence spectrometer with argon purged solution samples in 1cm cells. IR spectra were recorded on a Bio-Rad FTS-45 spectrometer with samples in compressed KBr-pellets. ^{1}H NMR spectra were recorded on Varian Mercury and Varian Gemini-2000 spectrometers (^{1}H at 199.97 MHz and 300.08 MHz, respectively). The chemical shifts are reported relative to residual solvent protons as reference. ^{99}Tc NMR spectra were recorded on a Varian Gemini-2000 spectrometer (^{99}Tc resonance 67.40 MHz), referenced to $[^{99}TcO_4]^-$. Electrospray ionisation mass spectra (ESI-MS) were recorded on a Merck Hitachi M-8000 spectrometer, reported are the values of the ^{187}Re isotope. Elemental analyses were performed on a Leco CHNS-932 elemental analyser. Electrochemical measurements were carried out in DMF containing 0.1M TBA PF_6 as conducting electrolyte. A Metrohm 757VA Computrace electrochemical analyser was used with a standard three-electrode setup of glassy carbon working

and auxiliary electrodes and a Ag/AgCl reference electrode. All potentials are given vs. Ag/AgCl (NHE +221mV). Gas chromatograms were recorded using a Varian CP-3800 gas chromatograph with helium as carrier gas. The permanent gases CO, N_2, O_2 and H_2 were separated by a 3m x 2mm column packed with Varian molecular sieve 13X. The gases were detected using a thermal conductivity detector (Varian). Calibrations were performed by the injection of known quantities of pure gases.

Photochemical carbon dioxide reductions. Reactions catalysed by $[Re(CO)_3(diimine)X]$ complexes were tested in 50 ml septum capped Schlenk tubes. Exact volumes were determined gravimetrically. 10 ml of a solution containing TEOA (1 M) and the catalyst (1 mM) in DMF were prepared, wrapped in black foil and degassed using a CO_2-purged Schlenk-line. The mixture was equilibrated under 1.5 bar CO_2 pressure for 15 min. and then transferred to a dark room for illumination. The light source was a Leica Pradovit S AF slide projector equipped with a 250W Osram Xenophot HLX lamp. The light was filtered by a 400 nm cut-off filter (Schott GG 400) before reaching the sample at 40cm distance from the projector. Light intensities illuminating the sample were determined by a TES 1332A luxmeter to be 46.000 lux. 100 µl gas samples were drawn from the headspace above the solution and injected into the GC-TCD gas analyser.

X-ray diffraction studies. Suitable crystals were covered with Paratone N oil, mounted on top of a glass fibre and immediately transferred to a Stoe IPDS diffractometer. Data was collected at 183(2) K using graphite-monochromated Mo radiation (0.71073 Å). Data was corrected for Lorentz and polarisation effects as well as for absorption. Structures were solved with direct methods using SHELXS-97[47] or SIR97[48] and were refined by full-matrix least-squares methods on F^2 with SHELXL-97[49]. ORTEP plots were generated by the PLATON software package[50] and are drawn at 50% probability. The crystal data and refinement parameters of the presented structures are summarized in Table 5 and the full data are available through the supplementary information.

Table 5

Acknowledgements

We would like to thank Prof. Jon Dilworth and his group for the possibility to carry out initial CO_2-reduction experiments at the Inorganic Chemistry Laboratory of the University of Oxford, Great Britain. H. C. Starck, Berlin, Germany, generously donated rhenium metal to support our research.

Captions

Scheme 1. Photocatalytic conversion of CO_2 to CO and variation of the catalyst

Scheme 2. Diimine ligands used for the synthesis of [ReBr(diimine)$(CO)_3$] complexes with the numbering of the corresponding complexes in brackets: 2,2'-bipyridine (bipy) (**1-7**); 1,10-phenanthroline (phen) (**8**); dipyrido[3,2-f:2',3'-h]quinoxaline (dpq) (**9**); dipyrido[3,2-a:2',3'-c]phenazine (dppz) (**10**); 2,2'-biquinoline (biq) (**11**); 2,2'-bipyridine-4,4'-dicarboxylic acid (H_2dcbipy) (**12**); 2,2'-bipyrimidine (bpm) (**13**); 1,10-phenanthroline-5,6-dione (phd) (**14**); 2,2'-azobispyridine (abpy) (**15**).

Figure 1. ORTEP drawing of one of the two independent molecules of [TcCl(bipy)$(CO)_3$] (**3**).

Figure 2. ORTEP representation of **10**, showing a view of the molecule from above and from the side.

Figure 3. ORTEP drawings of a top and a side view of **11**.

Figure 4. Absorption spectra for different [ReBr(diimine)$(CO)_3$] complexes in DMF (all solutions 0.2 mM).

Figure 5. Emission spectra for different [ReBr$(CO)_3$(diimine)] complexes in DMF (all solutions 0.2 mM).

Figure 6. ORTEP drawing of **14**, which contains a mirror plane going through Re1, Br1A and the ligand between the nitrogen atoms.

Figure 7. a) cyclic voltammogram of the two reversible reduction steps observed for **14** in DMF containing increasing concentrations of water. b) a scheme illustrating the successive reduction of the phd dione to form a semiquinone and then a diolate.

Figure 8. STERN- VOLMER plots for the fluorescence quenching of the excited states of different [ReX(diimine)$(CO)_3$] complexes by TEOA.

Figure 9. Formation of CO. Reactions with different [ReX(bipy)$(CO)_3$] and [TcCl(bipy)$(CO)_3$(bipy)]

Table 1. Spectroscopic and electrochemical properties of [ReX(bipy)$(CO)_3$] complexes.

Ligand X	λ_{max} [nm][a]	λ_{em} [nm][a]	ν_{CO} [cm^{-1}][b]	$E_{1/2,red}$ [mV][c]
Cl (**1**)	370	580	2019, 1883	-1130
Br (**2**)	370	575	2019, 1905	-1190
H_2O (**4**)	350	540	2036, 1918	-1000
SCN (**5**)	375	580	2020, 1928	-1015
CN (**6**)	355	540	2006, 1878	-1125
μ-CN-Re (**7**)	365	535	2025, 1910	-1050

[a] in DMF solution. [b] KBr pellets. [c] in DMF solution containing 0.1 M NBu_4PF_6.

Table 2. Spectroscopic and electrochemical properties of [ReBr(diimine)$(CO)_3$] complexes.

Diimine ligand	λ_{max} [nm][a]	λ_{em} [nm][a]	ν_{CO} [cm^{-1}][b]	$E_{1/2,red}$ [mV][c]
bipy (**2**)	370	575	2019, 1905	-1190
phen (**8**)	370	570	2018, 1933	-1090
dpq (**9**)	~375[d]	585	2025, 1948	-975
dppz (**10**)	~425[d]	520	2018, 1918	-705
biq (**11**)	435	/[e]	2014, 1895	-735
Hdcbipy (**12**)	360	540	2024, 1896	-1250[f]
bpm (**13**)	385	/[e]	2030, 1931	-860
phd (**14**)	375[d]	/[e]	2033, 1943	-15, -755
abpy (**15**)	550, 360[d]	/[e]	2020, 1924	+50

[a] in DMF solution. [b] KBr pellets. [c] in DMF solution containing 0.1 M NBu_4PF_6. [d] absorption shoulder. [e] no fluorescence observed at room temperature in DMF solution. [f] irreversible reduction.

Table 3. STERN- VOLMER constants determined by linear fits of the data forced through zero together with the corresponding values of $E_{1/2, red}$ and λ_{em}.

complex	K_{SV}	$E_{1/2, red}$ [mV]	λ_{em} [nm]
1	0.6	-1130	580
2	3.0	-1190	575
5	1.9	-1015	580
6	3.5	-1125	540
8	11.1	-1090	570
9	4.9	-975	585
10	13.5	-705	520
12	20.5	-1250	540

Table 4. Formation of CO for reactions of photocatalysts of the $[ReX(CO)_3(bipy)]$ series and $[TcCl(bipy)(CO)_3]$.

catalyst	CO after 30min. [eq./cat.]	CO after 120min. [eq./cat.]
1	4.6	8.2
2	4.0	13.0
3	1.6	5.5
4	0.5	1.8
5	4.9	26.4
6	1.1[a]	4.5
7	0.6[a]	2.6
8	4.8	11.5
9	0.5	1.1
12	2.2	7.7

[a] extrapolated values

Table 5. Crystal and Structure Refinement Data for **1**, **3**, **10**, **11** amd **14**

Compound No.	**1**	**3**	**10**	**11**	**14**
Formula	$C_{13}H_8ClN_2O_3Re$	$C_{13}H_8ClN_2O_3Tc$	$C_{21}H_{10}BrN_4O_3Re$	$C_{21}H_{12}BrN_2O_3Re$	$C_{15}H_6BrN_2O_5Re$
M_r	461.86	373.67	632.44	606.44	560.33
Crystal system	monoclinic	triclinic	triclinic	triclinic	orthorhombic
Space group	$P2_1/n$	P-1	P-1	P-1	Pnma
a/Å	6.8740(5)	10.9879(8)	6.9955(7)	7.5081(10)	7.2858(5)
b/Å	15.0038(9)	11.5003(9)	12.9547(11)	9.7573(10)	12.7348(6)
c/Å	13.5114(11)	11.1203(9)	13.2653(12)	12.9934(18)	16.7641(9)
α/°		93.703(10)	111.200(10)	94.697(15)	
β/°	96.494(10)	103.282(9)	98.272(11)	94.288(16)	
γ/°		86.214(9)	95.110(11)	106.434(14)	
V/Å^3	1384.57(17)	1362.87(18)	1096.10(17)	905.1(2)	1555.43(15)
Z	4	4	2	2	4
D_c/g cm^{-3}	2.216	1.821	1.916	2.225	2.393
□(Mo-Kα)/mm^{-1}	8.976	1.259	7.394	8.946	10.409
Goodness-of-fit on F^2	0.882	0.867	0.926	1.042	1.047
$R^{a,b}$	0.0464	0.0426	0.0593	0.0749	0.0701
$wR_2^{a,c}$	0.0702	0.0990	0.1685	0.1893	0.1835
Max., min. peaks/e·Å^{-3}	3.433, -1.822	0.661, -0.970	3.063, -1.710	2.066, -2.314	2.002, -1.804

[a] Observation criterion: $I > 2\sigma(I)$. [b] $R = \Sigma||F_o| - |F_c||/\Sigma|F_o|$. [c] $wR_2 = \{\Sigma[w(F_o^2 - F_c^2)^2]/\Sigma[w(F_o^2)^2]\}^{1/2}$

References

[1] K. Kalyanasundaram, *Photochemistry of Polypyridine and Porphyrin Complexes*, Academic Press, London, **1992**.
[2] V. Balzani, A. Juris, M. Venturi, S. Campagna, S. Serroni, *Chem. Rev.* **1996**, *96*, 759.
[3] M. Grätzel, *Nature* **2001**, *414*, 338.
[4] P. Wang, C. Klein, R. Humphry-Baker, S. M. Zakeeruddin, M. Grätzel, *J. Am. Chem. Soc.* **2005**, *127*, 808.
[5] M. Wrighton, D. L. Morse, *J. Am. Chem. Soc.* **1974**, *96*, 998.
[6] J. C. Luong, L. Nadjo, M. S. Wrighton, *J. Am. Chem. Soc.* **1978**, *100*, 5790.
[7] J. V. Caspar, T. J. Meyer, *J. Phys. Chem.* **1983**, *87*, 952.
[8] C. Kutal, M. A. Weber, G. Ferraudi, D. Geiger, *Organometallics* **1985**, *4*, 2161.
[9] K. Kalyanasundaram, *J. Chem. Soc., Faraday Trans. 2* **1986**, *82*, 2401.
[10] J. Hawecker, J. M. Lehn, R. Ziessel, *Helv. Chim. Acta* **1986**, *69*, 1990.
[11] W. Kaim, S. Kohlmann, *Chem. Phys. Lett.* **1987**, *139*, 365.
[12] D. J. Stufkens, *Comments Inorg. Chem.* **1992**, *13*, 359.
[13] H. Hori, J. Ishihara, K. Koike, K. Takeuchi, T. Ibusuki, O. Ishitani, *J. Photochem. Photobiol. A* **1999**, *120*, 119.
[14] Y. Hayashi, S. Kita, B. S. Brunschwig, E. Fujita, *J. Am. Chem. Soc.* **2003**, *125*, 11976.

[15] W. Hieber, H. Fuchs, *Z. Anorg. Allg. Chem.* **1941**, *248*, 269.
[16] A. Juris, S. Campagna, I. Bidd, J. M. Lehn, R. Ziessel, *Inorg. Chem.* **1988**, *27*, 4007.
[17] L. Wallace, D. P. Rillema, *Inorg. Chem.* **1993**, *32*, 3836.
[18] G. J. Kavarnos, *Fundamentals of Photoinduced Electron Transfer*, VCH, Weinheim, **1993**.
[19] J. Hawecker, J. M. Lehn, R. Ziessel, *J. Chem. Soc., Chem. Comm.* **1983**, 536.
[20] G. Calzaferri, K. Haedener, J. Li, *J. Photochem. Photobiol. A* **1992**, *64*, 259.
[21] C. Kutal, A. J. Corbin, G. Ferraudi, *Organometallics* **1987**, *6*, 553.
[22] H. Hartmann, W. Kaim, M. Wanner, A. Klein, S. Frantz, C. Duboc-Toia, J. Fiedler, S. Zalis, *Inorg. Chem.* **2003**, *42*, 7018.
[23] S. F. Haddad, J. A. Marshall, A. Crosby, B. Twamley, *Acta Cryst.* **2002**, *E58*, m559.
[24] Y. D. Chen, L. Y. Zhang, Z. N. Chen, *Acta Cryst.* **2005**, *E61*, m121.
[25] N. J. Lundin, P. J. Walsh, S. L. Howell, J. J. McGarvey, A. G. Blackman, K. C. Gordon, *Inorg. Chem.* **2005**, *44*, 3551.
[26] J. Guerrero, S. A. Moya, M. T. Garland, R. F. Baggio, *Acta Cryst.* **1999**, *C55*, 932.
[27] W. Kaim, *Coord. Chem. Rev.* **2001**, *219-221*, 463.
[28] J. Fees, W. Kaim, M. Moscherosch, W. Matheis, J. Klima, M. Krejcik, S. Zalis, *Inorg. Chem.* **1993**, *32*, 166.
[29] H. Hartmann, T. Scheiring, J. Fiedler, W. Kaim, *J. Organomet. Chem.* **2000**, *604*, 267.
[30] T. S. Eckert, T. C. Bruice, J. A. Gainor, S. M. Weinreb, *Proc. Natl. Acad. Sci. USA* **1982**, *79*, 2533.
[31] A. I. Krasna, *Photochem. Photobiol.* **1979**, *29*, 267.
[32] C. Pac, K. Ishii, S. Yanagida, *Chem. Lett.* **1989**, 765.
[33] S. P. Schmidt, W. C. Trogler, F. Basolo, *Inorg. Synth.* **1990**, *28*, 160.
[34] R. Alberto, A. Egli, U. Abram, K. Hegetschweiler, V. Gramlich, P. A. Schubiger, *J. Chem. Soc., Dalton Trans.* **1994**, 2815.
[35] R. Alberto, R. Schibli, P. A. Schubiger, U. Abram, T. A. Kaden, *Polyhedron* **1996**, *15*, 1079.
[36] D. Vitali, F. Calderazzo, *Gazz. Chim. Ital.* **1972**, *102*, 587.
[37] E. W. Abel, P. J. Heard, K. G. Orrell, *Inorg. Chim. Acta* **1997**, *255*, 65.
[38] S. A. Moya, J. Guerrero, R. Pastene, R. Sartori, R. Schmidt, R. Sariego, J. Sanz-Aparicio, I. Fonseca, M. Martinez-Ripoll, *Inorg. Chem.* **1994**, *33*, 2341.
[39] A. Kirpal, E. Reiter, *Chem. Ber.* **1927**, *60*, 664.
[40] R. van Belzen, R. A. Klein, W. J. J. Smeets, A. L. Spek, R. Benedix, C. J. Elsevier, *Recl. Trav. Chim. Pays Bas* **1996**, *115*, 275.
[41] J. E. Dickeson, L. A. Summers, *Austr. J. Chem.* **1970**, *23*, 1023.
[42] C. Hiort, P. Lincoln, B. Norden, *J. Am. Chem. Soc.* **1993**, *115*, 3448.
[43] B. Salignac, P. V. Grundler, S. Cayemittes, U. Frey, R. Scopelliti, A. E. Merbach, R. Hedinger, K. Hegetschweiler, R. Alberto, U. Prinz, G. Raabe, U. Kolle, S. Hall, *Inorg. Chem.* **2003**, *42*, 3516.
[44] A. M. B. Rodriguez, A. Gabrielsson, M. Motevalli, P. Matousek, M. Towrie, J. Sebera, S. Zalis, A. Vlcek, *J. Phys. Chem. A* **2005**, *109*, 5016.
[45] K. Kalyanasundaram, M. Grätzel, M. K. Nazeeruddin, *Inorg. Chem.* **1992**, *31*, 5243.
[46] S. Frantz, M. Weber, T. Scheiring, J. Fiedler, C. Duboc, W. Kaim, *Inorg. Chim. Acta* **2004**, *357*, 2905.
[47] G. M. Sheldrick, *Acta Cryst.* **1990**, *A46*, 467.
[48] A. Altomare, M. C. Burla, M. Camalli, G. L. Cascarano, C. Giacovazzo, A. Guagliardi, A. G. G. Moliterni, G. Polidori, R. Spagna, *J. Appl. Crystallogr.* **1999**, *32*, 115.
[49] G. M. Sheldrick, University Göttingen, **1997**.
[50] A. L. Spek, *J. Appl. Crystallogr.* **2003**, *36*, 7.

Schemes and Figures

Scheme 1.

Scheme 2.

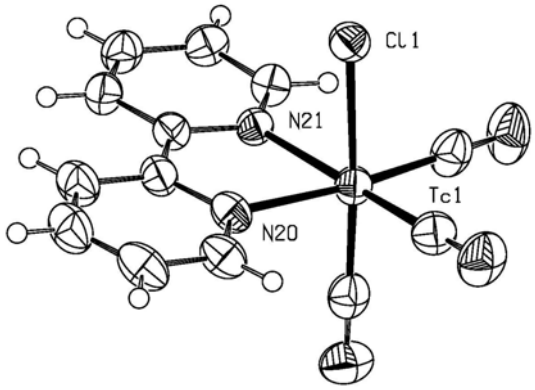

Figure 1.

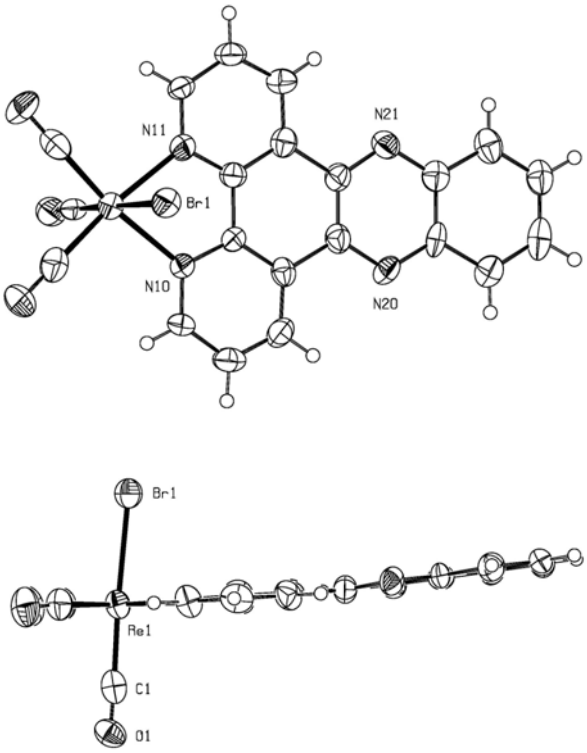

Figure 2.

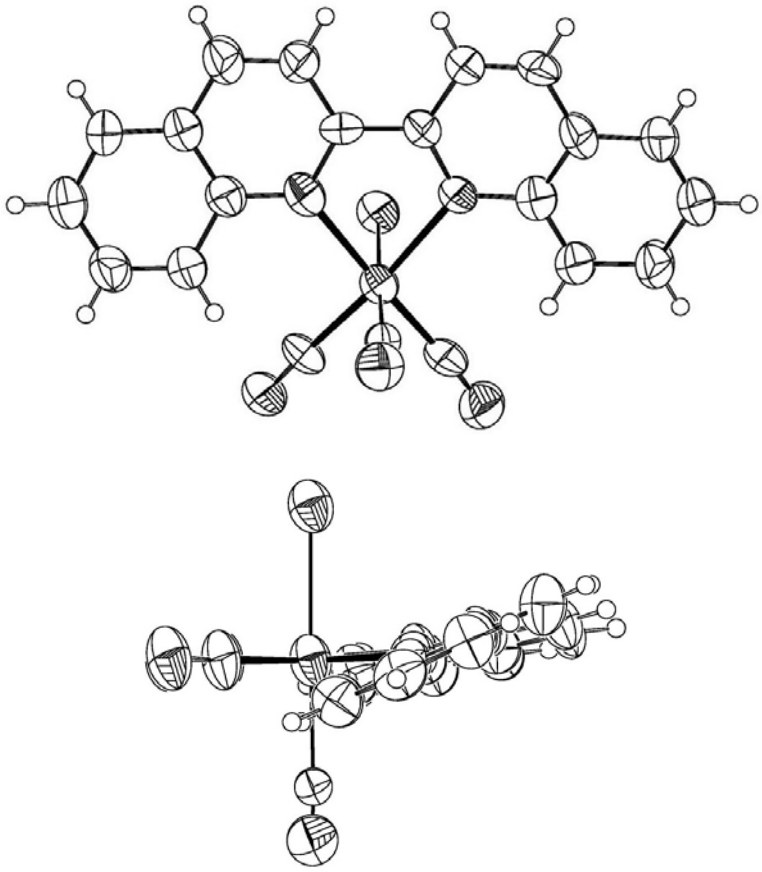

Figure 3.

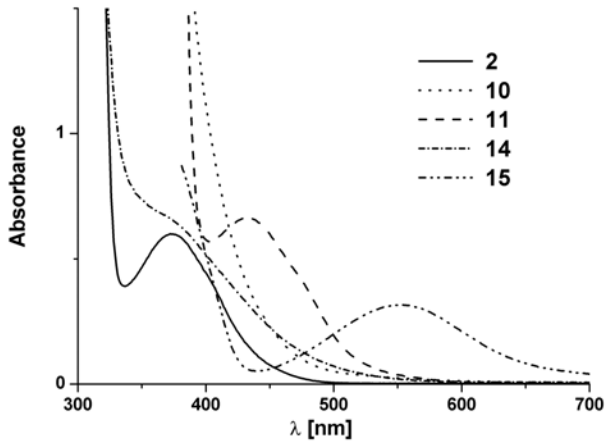

Figure 4.

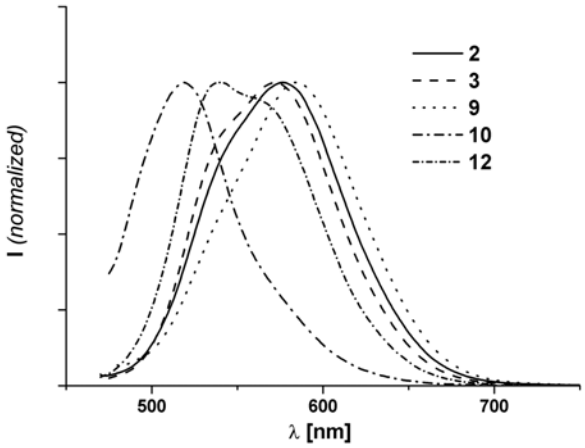

Figure 5.

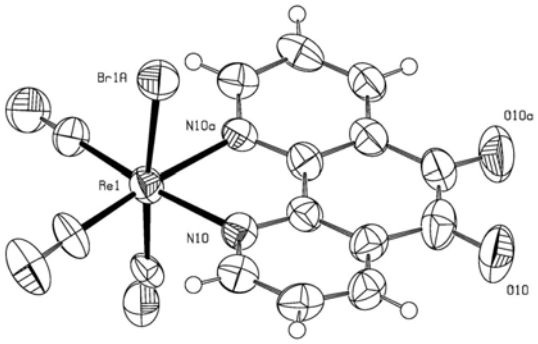

Figure 6.

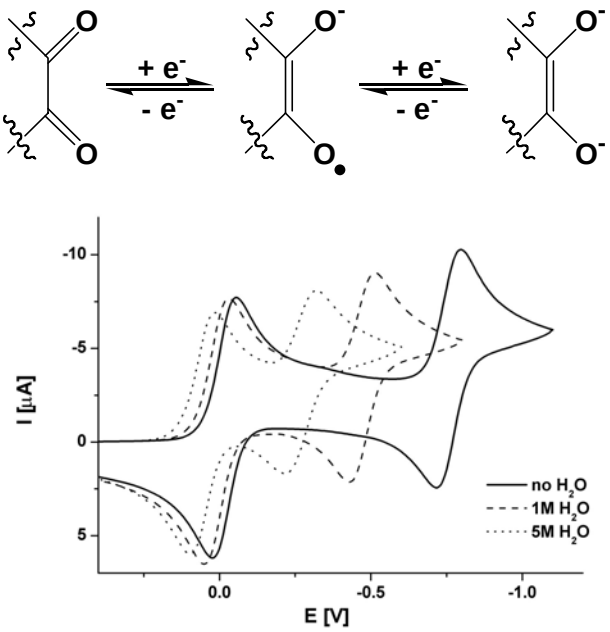

Figure 7.

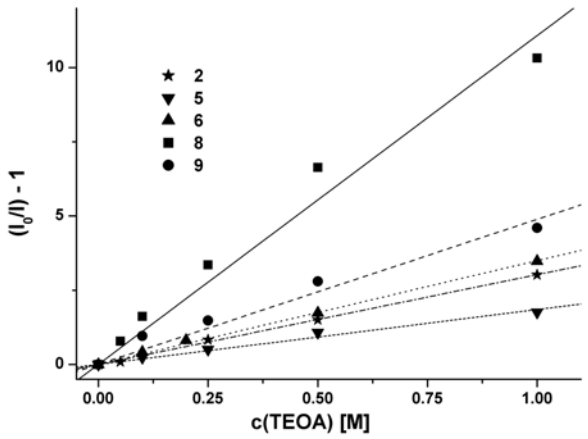

Figure 8.

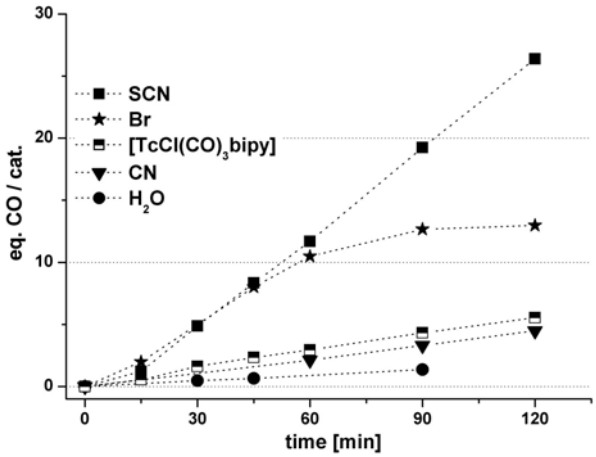

Figure 9.